

**Creating and detecting poor man's Majorana bound states in interacting quantum dots**Athanasios Tsintzis <sup>1</sup>, Rubén Seoane Souto <sup>1,2</sup> and Martin Leijnse<sup>1,2</sup><sup>1</sup>*Division of Solid State Physics and NanoLund, Lund University, S-221 00 Lund, Sweden*<sup>2</sup>*Center for Quantum Devices, Niels Bohr Institute, University of Copenhagen, DK-2100 Copenhagen, Denmark*

(Received 15 July 2022; revised 29 September 2022; accepted 27 October 2022; published 17 November 2022)

We propose and theoretically investigate an alternative way to create the poor man's Majorana bound states (MBSs) introduced in *Phys. Rev. B* **86**, 134528 (2012). Our proposal is based on two quantum dots (QDs) with strong electron-electron interactions that couple via a central QD with proximity-induced superconductivity. In the presence of spin-orbit coupling and a magnetic field, gate control of all three QDs allows tuning the system into sweet spots with one MBS localized on each outer dot. We quantify the quality of these MBSs and show how it depends on the Zeeman energy and interaction strength. We also show how nonlocal transport spectroscopy can be used to identify sweet spots with high MBS quality. Our results provide a path for investigating MBS physics in a setting that is free of many of the doubts and uncertainties that plague other platforms.

DOI: [10.1103/PhysRevB.106.L201404](https://doi.org/10.1103/PhysRevB.106.L201404)

**Introduction.** The realization of Majorana bound states (MBSs) [1–4] is one of the most heavily pursued goals in condensed matter physics. The motivation is their theoretically predicted nonabelian and nonlocal properties. In addition to being of fundamental interest as a new physics phenomenon, these properties allow for protected ways to store and manipulate quantum information [5]. The simplest toy model where MBSs arise is the Kitaev model [6], a tight-binding chain with spinless electrons and  $p$ -wave superconducting pairing. An explosion in experimental activities was motivated by various theoretical proposals showing that different quantum systems can be engineered such that the Kitaev model arises as an effective description of the low-energy degrees of freedom [7–13].

By now, experiments have revealed signatures consistent with MBSs in several of the proposed platforms, see Refs. [12,14–22] for a few examples. However, it has also become increasingly clear that the disorder that plagues all real materials can give rise to other, nontopological states that can provide an alternative explanation for most experimental observations [23–33]. So far, the nonabelian and nonlocal properties of MBSs have not been experimentally demonstrated.

One way to avoid the problem of imperfect materials is to engineer an artificial Kitaev chain in quantum dots (QDs) coupled via narrow superconducting regions [34]. In fact, it was shown in Ref. [35] that two QDs are enough to obtain MBSs, named poor man's MBSs because they possess all the properties of MBSs but only exist at fine-tuned sweet spots in parameter space. The poor man's MBSs system closely

resembles Cooper pair splitter devices [36–39], but requires both strong crossed Andreev reflection (CAR) and the ability to fine-tune either the spin-orbit coupling strength or the angle between noncollinearly polarized QD spins. In addition, given the lack of topological protection, it is unclear how close one can come to ideal MBSs in a realistic system with finite Zeeman energy and electron-electron interactions on the QDs.

In this work, we show a way to overcome the difficulties and uncertainties associated with the original proposal for poor man's MBSs. A key ingredient is to couple the QDs via a central QD which is, in turn, strongly proximitized by a superconductor. The advantage is that gating the central QD provides control of the relative amplitudes of CAR and elastic cotunneling (ECT), which allows realizing the poor man's MBSs with a constant spin-orbit coupling (or a constant finite angle between the effective magnetic fields on the two QDs). The underlying physics is the same as a recent proposal for coupling the QDs via an Andreev bound state [40]. We analyze the role of finite Zeeman splitting (including both spin states on all three QDs) as well as strong Coulomb interactions. We show that sweet spots in parameter space exist where the system exhibits three characteristics that are prerequisites for MBSs with nonabelian properties as follows: (i) degenerate even and odd (electron number) parity ground states; (ii) a substantial gap to the excited states; and (iii) localized MBSs of high quality, which we quantify with the Majorana polarization (MP) [41–43]. Our results also show how the MP depends on the interaction strength and Zeeman energy. This is important because there are regions in parameter space associated with apparent sweet spots that fulfill (i) and (ii), but have poor MP. Finally, we calculate the nonlocal transport signatures of the interacting system and show that they can be used to identify sweet spots and distinguish between true sweet spots and apparent sweet spots with low MP.

While finalizing the present paper, a report of experimental signatures consistent with poor man's MBSs appeared [44] based on the Andreev bound state coupling proposed in Ref. [40]. The experiments were compared with a noninter-

---

*Published by the American Physical Society under the terms of the Creative Commons Attribution 4.0 International license. Further distribution of this work must maintain attribution to the author(s) and the published article's title, journal citation, and DOI. Funded by Bibsam.*

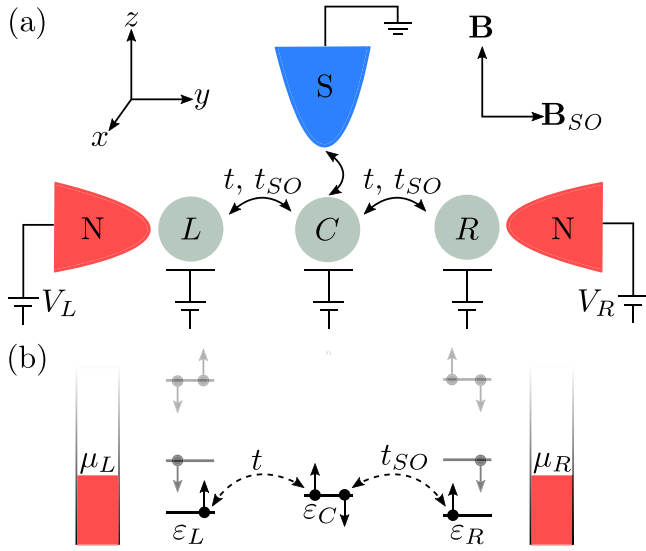


FIG. 1. (a) Setup with three QDs ( $L, C, R$ ) coupled via spin-conserving tunneling  $t$  and (spin-orbit-induced) spin-flip tunneling  $t_{SO}$ . QD  $C$  is strongly coupled to a grounded superconductor.  $\mathbf{B}$  is an external Zeeman field and  $\mathbf{B}_{SO}$  is a spin-orbit field. (b) QD orbitals  $\varepsilon_j$  and examples of tunnel processes. Electron-electron interactions increase the energy cost of occupying a QD with two electrons. Two normal leads with chemical potentials  $\mu_{L,R}$  (controlled by voltages  $V_{L,R}$ ) couple to QDs  $L$  and  $R$  and can be used for tunnel spectroscopy.

acting model with infinite Zeeman energy, similar to Ref. [35]. The ground-state properties of interacting double QDs harboring poor man's MBSs were also investigated in Refs. [45–47].

*Proposed device and model.* To create and detect poor man's MBSs, we propose a device with three coupled QDs. The setup is shown in Fig. 1(a), while Fig. 1(b) shows a sketch of the involved energies and tunnel processes. The system is described by the Hamiltonian [excluding for now the normal ( $N$ ) leads]

$$\begin{aligned}
 H_{\text{QDs}} = & \sum_{\sigma,j} \varepsilon_j n_{j\sigma} + \sum_j U_j n_{j\uparrow} n_{j\downarrow} + \sum_j E_{Zj} n_{j\downarrow} \\
 & + \sum_{\sigma,j \neq C} [t_j d_{j\sigma}^\dagger d_{C\sigma} + \text{H.c.}] \\
 & + \sum_{j \neq C} [t_j^{\text{SO}} d_{j\uparrow}^\dagger d_{C\downarrow} - t_j^{\text{SO}} d_{j\downarrow}^\dagger d_{C\uparrow} + \text{H.c.}] \\
 & + \Delta [d_{C\uparrow}^\dagger d_{C\downarrow}^\dagger + \text{H.c.}]. \quad (1)
 \end{aligned}$$

Here,  $d_{j\sigma}^\dagger$  creates an electron with spin  $\sigma = \uparrow, \downarrow$  in QD  $j = L, C, R$  with occupation  $n_{j\sigma} = d_{j\sigma}^\dagger d_{j\sigma}$ , single-particle orbital energy  $\varepsilon_j$ , charging energy  $U_j$ , and Zeeman energy  $E_{Zj}$ .  $t_j$  is the amplitude for spin-conserving tunneling between QDs  $j = L, R$  and QD  $C$ , while  $t_j^{\text{SO}}$  is the amplitude for spin-flip tunneling, which results from a spin-orbit interaction with spin-orbit field  $\mathbf{B}_{SO}$  along the  $y$ -axis, perpendicular to the external Zeeman field  $\mathbf{B}$  chosen here to be along the  $z$ -axis [48]. We include the proximity-induced superconductivity on QD  $C$  through a pairing term of amplitude  $\Delta$ , which is a reasonable approximation for energies below the superconducting gap [49–52].

*Relation to the original poor man's MBS model.* In the original model for poor man's MBSs [35], a superconductor mediates two different types of couplings between two fully spin-polarized QDs: CAR and ECT — corresponding, respectively, to the pairing and hopping terms in the Kitaev model [6]. The CAR and ECT amplitudes scale in the same way with the QD-superconductor coupling strength, but their ratio can be controlled via the angle between the QD spins. The MBS sweet spot occurs when the CAR and ECT amplitudes are equal and both QD levels are at zero energy (i.e., aligned with the chemical potential of the superconductor). At this point, the Kitaev chain hosts one MBS fully localized on each end site; then two sites — or two QDs — suffice to have spatially separated MBSs.

The relation between  $H_{\text{QDs}}$  in Eq. (1) and the simple poor man's MBS model is most easily understood in the regime where  $|\varepsilon_j|, |t_j|, |t_j^{\text{SO}}|, |E_{ZC}| \ll |\Delta|, |E_{ZL,R}|$  (although our future analyses will not be limited to this regime). Then, in the ground state, QDs  $L$  and  $R$  are occupied by zero or one electron each, while QD  $C$  is in a superposition of empty and doubly occupied (single occupation being suppressed by the large superconducting pairing). Second-order perturbation theory in  $t_j$  and  $t_j^{\text{SO}}$  gives a coupling between QDs  $L$  and  $R$ , both through ECT ( $\propto t_L t_R$ ) and CAR ( $\propto t_L t_R^{\text{SO}} + t_R t_L^{\text{SO}}$ , as the singlet nature of the Cooper pairs means that a spin flip is needed to populate the lowest spin state of each QD).  $H_{\text{QDs}}$  conserves the parity (even or odd) of the total electron number. Couplings within the even (odd) parity sector are mediated by CAR (ECT) which therefore lowers the energy of the even (odd) parity ground state. However, because of interference between different tunnel processes, the amplitudes of CAR and ECT depend differently on  $\varepsilon_C$ , such that ECT is suppressed around  $\varepsilon_C = 0$ . A similar control of the CAR and ECT relative amplitudes can be achieved using a closely related model with an Andreev bound state mediating the coupling between two QDs, as proposed in Ref. [40] and exploited in the experiments presented in Refs. [44,53].

Based on the original poor man's MBS model, a sweet spot is expected when the ECT and CAR amplitudes are equal and  $\varepsilon_L = \varepsilon_R = 0$ . To some degree this still holds in our model for finite  $E_{Zj}$  and  $U_j$ , but we need to compensate for renormalizations of  $\varepsilon_{L,R}$  due to the coupling to QD  $C$ . Away from the perturbative regime (in  $t_j, t_j^{\text{SO}}$ ), the concepts of CAR and ECT are no longer well defined, but the processes coupling states within the even parity sector and within the odd parity sector still depend differently on  $\varepsilon_C$ .

*Sweet spots and MBS quality.* Throughout the rest of the paper we, for simplicity, consider a symmetric system  $t_L = t_R = t, t_L^{\text{SO}} = t_R^{\text{SO}} = t_{SO}, U_L = U_R = U, E_{ZL} = E_{ZR} = E_Z$ . We assume that the strong coupling of QD  $C$  to the grounded superconductor quenched its charging energy by a combination of capacitive effects and tunnel-induced renormalization and reduced its Zeeman splitting (because of the small  $g$ -factor of the superconductor). We therefore take  $U_C = E_C = 0$ , but verified that relaxing these assumptions does not qualitatively change the results, see the Supplemental Material (SM) [54]. Unless otherwise stated, we choose the following values for the remaining parameters ( $e = \hbar = k_B = 1$ ):  $U = 5\Delta, t = 0.5\Delta, t_{SO} = 0.2t, E_Z = 1.5\Delta$ .

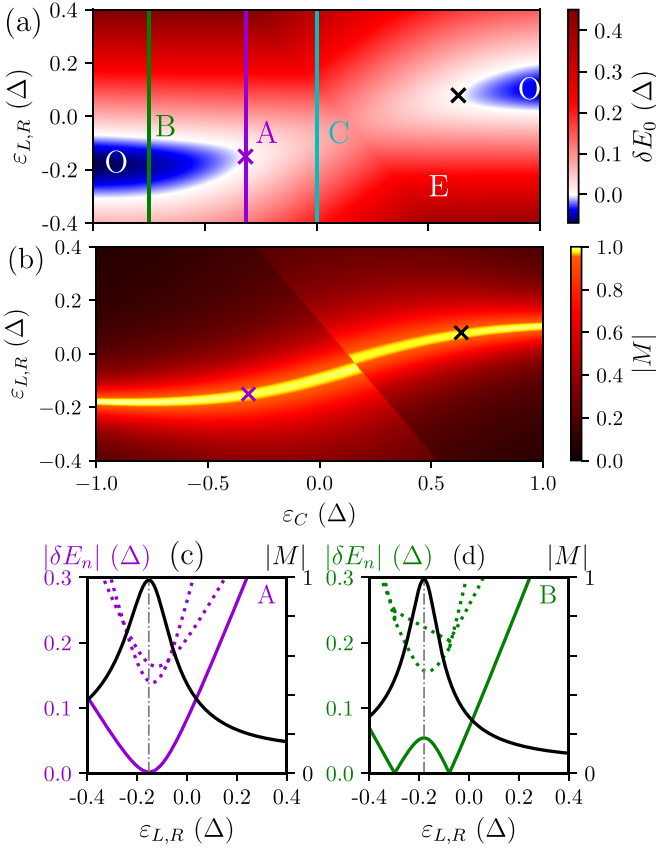


FIG. 2. (a)  $\delta E_0$  as a function of  $\epsilon_L = \epsilon_R$  and  $\epsilon_C$ . Cuts marked A, B, and C are explored in (c, d) and in Fig. 3, while O and E mark regions where the global ground state has odd and even parity, respectively. The purple cross marks the  $\epsilon_C < 0$  sweet spot at  $\epsilon_C \approx -0.319\Delta$ ,  $\epsilon_L = \epsilon_R \approx -0.151\Delta$ , while the  $\epsilon_C > 0$  sweet spot is marked by the black cross at  $\epsilon_C \approx 0.634\Delta$ ,  $\epsilon_L = \epsilon_R \approx 0.0785\Delta$ . (b)  $|M|$  as a function of  $\epsilon_L = \epsilon_R$  and  $\epsilon_C$ . The crosses mark the same points as in (a). (c)  $|\delta E_n|$  (left axis, purple lines) as a function of  $\epsilon_L = \epsilon_R$  along cut A (purple line) in (a). The lowest excited state (full line) has different parity (odd in this case) than the ground state (even in this case); one of the two higher excited states shown (dotted lines) has even parity and the other odd. The black line shows  $|M|$  (right axis) as a function of  $\epsilon_L = \epsilon_R$  along cut A in (a). (d) Same as (c) but along cut B (green line) in (a). The vertical dash-dotted lines in (c) and (d) indicate the maximum of  $|M|$ .

We first focus on  $\delta E_0 = E^O - E^E$ , the energy difference between the odd and even parity ground states of  $H_{\text{QDs}}$  in Eq. (1). As explained above,  $\epsilon_C$  affects the even and odd ground-state energies by changing the relative strengths of couplings within the even and odd parity sectors. For  $|\epsilon_C| < |\Delta|$  and  $\epsilon_L = \epsilon_R$ , the ground state is dominated by an even electron number on QD C. For large positive  $\epsilon_{L,R}$ , QDs L and R are both mainly empty and the global ground state of all three QDs thus has even parity. For negative  $\epsilon_{L,R}$  with  $|\epsilon_{L,R}| < U$ , the global ground state is also even because it is dominated by single occupations of both QDs L and R.

The above behavior is seen in Fig. 2(a), which shows  $\delta E_0$  as a function of  $\epsilon_C$  and  $\epsilon_L = \epsilon_R$ . When changing  $\epsilon_{L,R}$  along a vertical cut we start and end with an even parity ground state, but if  $|\epsilon_C|$  is large enough there is a region in between

with an odd parity ground state [blue color in Fig. 2(a)]. This happens for values of  $\epsilon_C$  such that couplings within the odd parity sector are stronger than those within the even parity sector. There are two values of  $\epsilon_C$  where this region reduces to a point as a function of  $\epsilon_{L,R}$  [marked with purple and black crosses in Fig. 2(a)] and we will see that these points are the closest we come to sweet spots with MBSs.

From Fig. 2(a) we see that we have lines in parameter space with degenerate even and odd parity ground states (white color). To determine whether these degeneracies are associated with MBSs, we quantify the MBS quality using the MP [41]. In our case, it corresponds to the degree that a Hermitian operator localized on one of the outer QDs  $j \neq C$  can switch between the lowest-energy even and odd states

$$M_j = \frac{\sum_{\sigma} (w_{\sigma}^2 - z_{\sigma}^2)}{\sum_{\sigma} (w_{\sigma}^2 + z_{\sigma}^2)}, \quad (2)$$

$$w_{\sigma} = \langle O | (d_{j\sigma} + d_{j\sigma}^{\dagger}) | E \rangle, \quad (3)$$

$$z_{\sigma} = \langle O | (d_{j\sigma} - d_{j\sigma}^{\dagger}) | E \rangle, \quad (4)$$

where  $|E\rangle$  ( $|O\rangle$ ) is the lowest-energy even (odd) parity state. This definition guarantees that  $0 \leq |M_j| \leq 1$ , where  $|M_j| = 1$  would indicate a single MBS perfectly localized on QD  $j$ , with no other MBS operator having any weight there. For the presented results,  $M_L = -M_R$  and in the following we drop the index  $j$  and focus on  $|M_L| = |M_R| = |M|$

Figure 2(b) shows  $|M|$  plotted over the same range in  $\epsilon_C$  and  $\epsilon_L = \epsilon_R$  used in Fig. 2(a). There is a line where  $|M|$  comes very close to 1, but this line only coincides with an even-odd degeneracy at two isolated points (marked with purple and black crosses). The discontinuity in  $|M|$  arises because the two lowest-energy odd-parity states undergo a crossing. This turns into an avoided crossing for  $\epsilon_L \neq \epsilon_R$  and occurs in a regime far from even/odd ground-state degeneracy where the MP has little meaning.

Figures 2(c) and 2(d) show  $|M|$  together with  $|\delta E_0|$  and the excitation energies above the global ground state ( $|\delta E_n|$ ,  $n \geq 1$ ) as a function of  $\epsilon_L = \epsilon_R$  for two different values of  $\epsilon_C$  [purple and green cuts in Fig. 2(a)]. Along both cuts, we find even/odd degeneracies with a substantial separation to excited states. However, it is only in Fig. 2(c) that this degeneracy coincides with a large  $|M|$  ( $\approx 0.986$ ), while in Fig. 2(d) the peak in  $|M|$  lies in between the two degeneracy points. Similar results are found for the region where  $\epsilon_C > 0$ .

We also investigate another important property of the MBSs in our system, namely, their chargeless nature. For that purpose, we calculate

$$\delta Q_{L,R} = \langle O | n_{L,R} | O \rangle - \langle E | n_{L,R} | E \rangle, \quad (5)$$

i.e., the lowest-energy even and odd parity states have a charge difference  $\delta Q_j$  on QD  $j$ . At the sweet spots in Fig. 2 we find  $|\delta Q_{L,R}| \approx 5 \times 10^{-3}$ , with significantly larger values away from the sweet spots. In summary, based on our results above, we draw the important conclusion that it is indeed possible to find sweet spots with localized MBSs in our system.

*Transport spectroscopy.* Next we focus on how to experimentally find the sweet spots with significant MP based on transport spectroscopy. We consider a transport setup according to Fig. 1(a) with QDs L and R coupled with tunnel

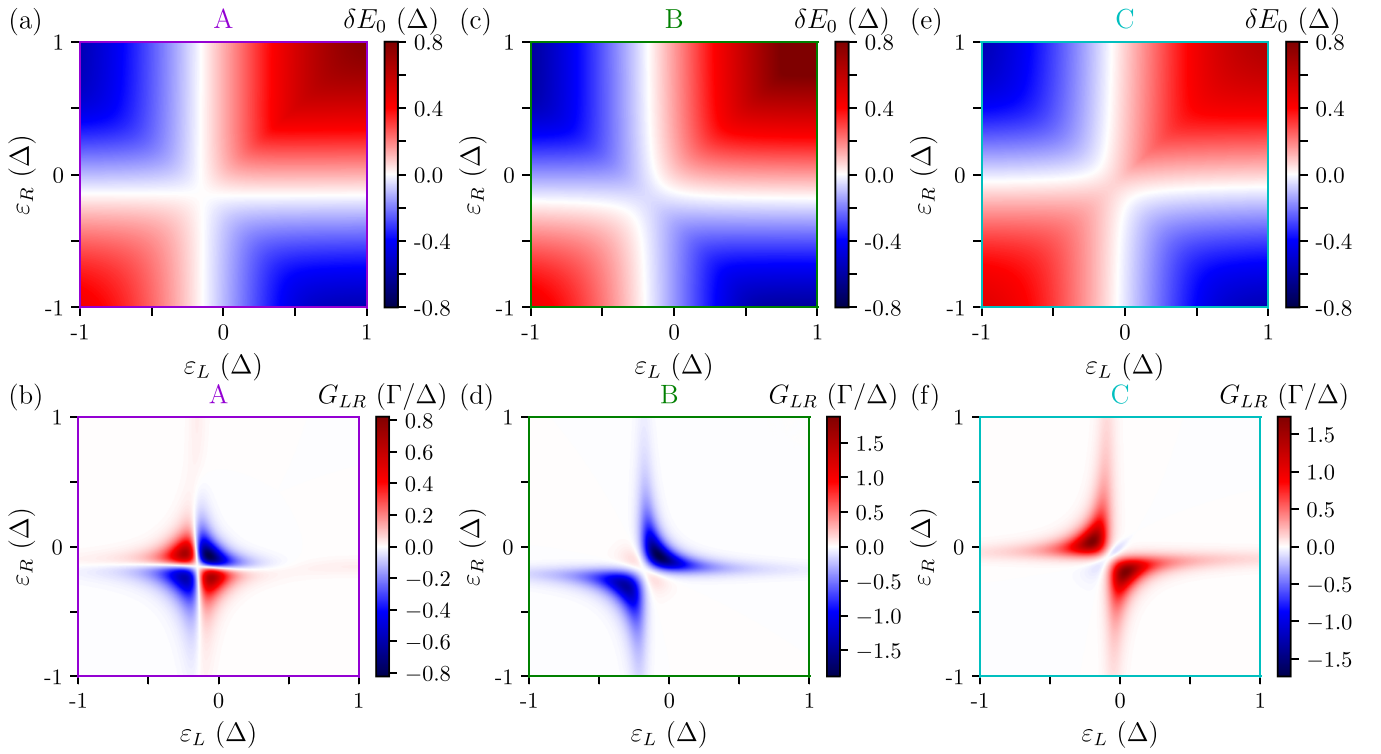


FIG. 3. (a), (c), and (e) Energy difference  $\delta E_0$  between even and odd parity ground states as a function of  $\varepsilon_L$  and  $\varepsilon_R$ , with the same  $\varepsilon_C$  as in the lines marked (a) A, (c) B, and (e) C in Fig. 2(a). (b), (d), and (f) Same as (a), (c), and (e), but showing  $G_{LR}$  instead.

couplings  $\Gamma_L = \Gamma_R = \Gamma$  to normal leads with applied voltages  $V_L$  and  $V_R$  (the superconductor is kept grounded). The normal leads are kept at temperature  $T = \Delta/40$ . Focusing on the regime  $\Gamma \ll T$ , we calculate the current based on first-order rate equations [54,55]. In this regime, Kondo correlations and renormalization of the QD energies due to the coupling to the normal leads are negligible.

Figures 3(a), 3(c), and 3(e) show  $\delta E_0$ , just as in Fig. 2(a), but now as a function of  $\varepsilon_L$  and  $\varepsilon_R$  with  $\varepsilon_C$  as in the lines marked A [Fig. 3(a)], B [Fig. 3(c)], and C [Fig. 3(e)] in Fig. 2(a). The local zero-bias conductance  $G_{jj} = dI_j/dV_j$  at  $V_L = V_R = 0$  is plotted in the SM [54] and shows peaks along the even-odd degeneracy lines. However, depending on  $T$  relative to the gap to excited states, it can be hard to accurately determine the sweet spot based on a local conductance measurement. It is known that nonlocal conductance, for example,  $G_{LR} = dI_L/dV_R$ , can reveal additional information about subgap states [56–59]. Figures 3(b), 3(d), and 3(f) show  $G_{LR}$  corresponding to the parameters in Figs. 3(a), 3(c), and 3(e). The MBS sweet spot, present only in Fig. 3(b), gives rise to a distinct  $G_{LR}$  texture, with  $G_{LR} = 0$  at the degeneracy lines which cross at the sweet spot, and equal magnitudes of positive and negative  $G_{LR}$ . In contrast, for parameters where there is no sweet spot, zeros of  $G_{LR}$  do not coincide with degeneracy lines and  $G_{LR}$  is dominated by either positive or negative values. This is in qualitative agreement with the experimental findings in Ref. [44].

*Low-quality MBSs.* Finally, we investigate how the MBS quality, as quantified by the MP, depends on the different parameters, and how we can avoid being fooled by an apparent sweet spot with low MP (“low-MP sweet spot” in the follow-

ing). Figure 4(a) shows  $|M|$  as a function of  $E_Z = E_{ZL} = E_{ZR}$  for different values of  $U$  with  $\varepsilon_C$  and  $\varepsilon_L = \varepsilon_R$  adjusted to an even-odd degeneracy with the highest possible  $|M|$  (all other parameters are the same as above). For large  $E_Z$  we find that  $|M| \rightarrow 1$ , which is to be expected as the model

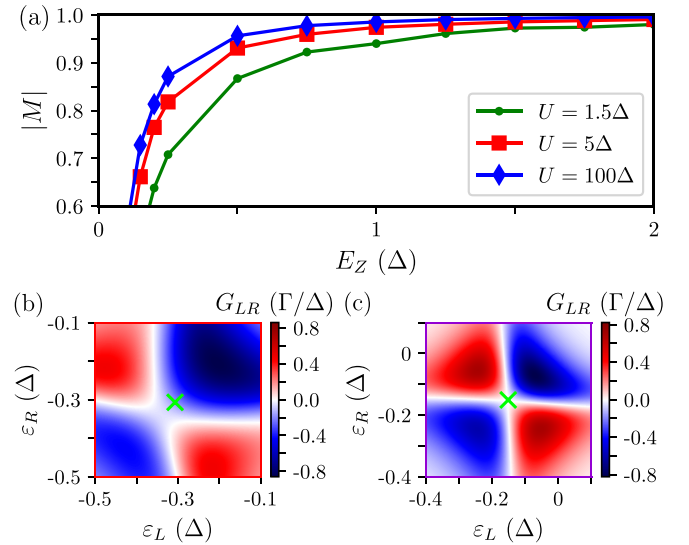


FIG. 4. (a)  $|M|$  as a function of  $E_Z$  for different  $U$ . (b)  $G_{LR}$  as a function of  $\varepsilon_L$  and  $\varepsilon_R$  for  $E_Z = 0.15\Delta$  and  $U = 5\Delta$ . There is an apparent sweet spot at  $\varepsilon_C \approx -0.558\Delta$ ,  $\varepsilon_L = \varepsilon_R \approx -0.316\Delta$  (marked with a green cross) with a low  $|M| \approx 0.661$ . (c) Same as (b) but for the same parameters as in Fig. 3(a) [zoomed in version of Fig. 3(a)]. At the sweet spot marked with the green cross in (c),  $|M| \approx 0.985$ .

then approaches the original poor man's MBS model [35]. Importantly, however, we note that the values of  $E_Z$  required for a good MP are much larger than the gap to the nearest excited states which is  $\sim 0.15\Delta$  in Fig. 2(c). A large  $U$  helps to maintain high MP for smaller  $E_Z$ , which is also to be expected as it suppresses local Andreev reflection and prevents double occupation of the outer QDs.

The appearance of low-MP sweet spots presents a challenge for experiments aiming to identify and eventually utilize MBSs. Figure 4(a) shows what to expect for a given set of parameters, but a direct experimental signature that can distinguish between high- and low-MP sweet spots would be desirable. As we show in the SM [54],  $\delta E_0(\varepsilon_L, \varepsilon_R, \varepsilon_C)$  (and therefore the local conductances) are rather similar for high- and low-MP sweet spots. We also find a similarly small  $\delta Q$  [see Eq. (5)] for high- and low-MP sweet spots. Fortunately, a distinction can, in principle, be made based on a measurement of  $G_{LR}$ . Figure 4(b) shows  $G_{LR}$  for parameters such that the MP maximum is  $|M| \approx 0.661$ , while Fig. 4(c) shows the same plot for parameters such that the MP maximum is  $|M| \approx 0.985$ . For relatively low  $|M|$  the zero lines in  $G_{LR}$  do not cross, and the avoided crossing does not coincide with the location of the low-MP sweet spot (marked with a green cross). The nonlocal conductance is thus finite at the degeneracy.

*Conclusions.* In this work, we considered a system with three QDs for engineering fine-tuned MBSs, the so-called poor man's MBSs. These states require proximity-induced

superconductivity on the central QD, spin-orbit coupling between the QDs, Zeeman splitting due to an external field, and fine-tuning of the energies of the QD orbitals. We quantified the MBS quality using the MP, showing that onsite Coulomb repulsion in the outer dots and Zeeman field increase their quality. A good MBS is characterized by the simultaneous occurrence of a degenerate ground state and a high MP value for the same parameters. In contrast, a bad MBS shows low MP values at the ground-state degeneracy. This characteristic leads to different nonlocal transport properties, which can be used to identify high-quality MBSs.

Although the poor man's MBSs are not topologically protected, they preserve the remaining topological properties, including the nonabelian exchange properties. For this reason, they become a promising alternative to experimentally demonstrate the exotic physics of MBSs. Proposals to measure noise [60–63] or entropy [64–67] associated with MBSs, and to measure Majorana fusion [68,69] and braiding [70–72] are compatible with the present proposal, allowing for a definitive demonstration of the topological superconducting phase.

*Acknowledgments.* We acknowledge stimulating discussions with M. Nitsch, V. Svensson, O. A. Awoga, S. Matern, A. Danilenko, A. Pöschl, K. Flensberg, and C. M. Marcus, and funding from NanoLund, the Swedish Research Council (VR) and the European Research Council (ERC) under the European Unions Horizon 2020 research and innovation programme under Grant Agreement No. 856526.

- 
- [1] J. Alicea, *Rep. Prog. Phys.* **75**, 076501 (2012).
- [2] M. Leijnse and K. Flensberg, *Semicond. Sci. Technol.* **27**, 124003 (2012).
- [3] R. Aguado, *Riv. Nuovo Cimento* **40**, 523 (2017).
- [4] C. W. J. Beenakker, *SciPost Phys. Lect. Notes* **1**, 15 (2020).
- [5] C. Nayak, S. H. Simon, A. Stern, M. Freedman, and S. Das Sarma, *Rev. Mod. Phys.* **80**, 1083 (2008).
- [6] A. Y. Kitaev, *Phys. Usp.* **44**, 131 (2001).
- [7] R. M. Lutchyn, J. D. Sau, and S. Das Sarma, *Phys. Rev. Lett.* **105**, 077001 (2010).
- [8] Y. Oreg, G. Refael, and F. von Oppen, *Phys. Rev. Lett.* **105**, 177002 (2010).
- [9] S. Nadj-Perge, I. K. Drozdov, B. A. Bernevig, and A. Yazdani, *Phys. Rev. B* **88**, 020407(R) (2013).
- [10] M. Hell, M. Leijnse, and K. Flensberg, *Phys. Rev. Lett.* **118**, 107701 (2017).
- [11] F. Pientka, A. Keselman, E. Berg, A. Yacoby, A. Stern, and B. I. Halperin, *Phys. Rev. X* **7**, 021032 (2017).
- [12] S. Vaitiekėnas, G. W. Winkler, B. van Heck, T. Karzig, M.-T. Deng, K. Flensberg, L. I. Glazman, C. Nayak, P. Krogstrup, R. M. Lutchyn, and C. M. Marcus, *Science* **367**, eaav3392 (2020).
- [13] K. Flensberg, F. von Oppen, and A. Stern, *Nat. Rev. Mater.* **6**, 944 (2021).
- [14] V. Mourik, K. Zuo, S. M. Frolov, S. R. Plissard, E. P. A. M. Bakkers, and L. P. Kouwenhoven, *Science* **336**, 1003 (2012).
- [15] M. T. Deng, C. L. Yu, G. Y. Huang, M. Larsson, P. Caroff, and H. Q. Xu, *Nano Lett.* **12**, 6414 (2012).
- [16] A. D. K. Finck, D. J. Van Harlingen, P. K. Mohseni, K. Jung, and X. Li, *Phys. Rev. Lett.* **110**, 126406 (2013).
- [17] S. Nadj-Perge, I. K. Drozdov, J. Li, H. Chen, S. Jeon, J. Seo, A. H. MacDonald, B. A. Bernevig, and A. Yazdani, *Science* **346**, 602 (2014).
- [18] M. T. Deng, S. Vaitiekėnas, E. B. Hansen, J. Danon, M. Leijnse, K. Flensberg, J. Nygård, P. Krogstrup, and C. M. Marcus, *Science* **354**, 1557 (2016).
- [19] F. Nichele, A. C. C. Drachmann, A. M. Whiticar, E. C. T. O'Farrell, H. J. Suominen, A. Fornieri, T. Wang, G. C. Gardner, C. Thomas, A. T. Hatke, P. Krogstrup, M. J. Manfra, K. Flensberg, and C. M. Marcus, *Phys. Rev. Lett.* **119**, 136803 (2017).
- [20] R. M. Lutchyn, E. P. Bakkers, L. P. Kouwenhoven, P. Krogstrup, C. M. Marcus, and Y. Oreg, *Nat. Rev. Mater.* **3**, 52 (2018).
- [21] A. Fornieri, A. M. Whiticar, F. Setiawan, E. Portolés, A. C. C. Drachmann, A. Keselman, S. Gronin, C. Thomas, T. Wang, R. Kallagher, G. C. Gardner, E. Berg, M. J. Manfra, A. Stern, C. M. Marcus, and F. Nichele, *Nature (London)* **569**, 89 (2019).
- [22] H. Ren, F. Pientka, S. Hart, A. T. Pierce, M. Kosowsky, L. Lunczer, R. Schlereth, B. Scharf, E. M. Hankiewicz, L. W. Molenkamp, B. I. Halperin, and A. Yacoby, *Nature (London)* **569**, 93 (2019).
- [23] E. Prada, P. San-Jose, and R. Aguado, *Phys. Rev. B* **86**, 180503(R) (2012).
- [24] G. Kells, D. Meidan, and P. W. Brouwer, *Phys. Rev. B* **86**, 100503(R) (2012).

- [25] J. Liu, A. C. Potter, K. T. Law, and P. A. Lee, *Phys. Rev. Lett.* **109**, 267002 (2012).
- [26] C.-X. Liu, J. D. Sau, T. D. Stanescu, and S. Das Sarma, *Phys. Rev. B* **96**, 075161 (2017).
- [27] C. Moore, C. Zeng, T. D. Stanescu, and S. Tewari, *Phys. Rev. B* **98**, 155314 (2018).
- [28] C. Reeg, O. Dmytruk, D. Chevallier, D. Loss, and J. Klinovaja, *Phys. Rev. B* **98**, 245407 (2018).
- [29] O. A. Awoga, J. Cayao, and A. M. Black-Schaffer, *Phys. Rev. Lett.* **123**, 117001 (2019).
- [30] A. Vuik, B. Nijholt, A. R. Akhmerov, and M. Wimmer, *SciPost Phys.* **7**, 061 (2019).
- [31] H. Pan and S. Das Sarma, *Phys. Rev. Res.* **2**, 013377 (2020).
- [32] E. Prada, P. San-Jose, M. W. A. de Moor, A. Geresdi, E. J. H. Lee, J. Klinovaja, D. Loss, J. Nygård, R. Aguado, and L. P. Kouwenhoven, *Nat. Rev. Phys.* **2**, 575 (2020).
- [33] R. Hess, H. F. Legg, D. Loss, and J. Klinovaja, *Phys. Rev. B* **104**, 075405 (2021).
- [34] J. D. Sau and S. D. Sarma, *Nat. Commun.* **3**, 964 (2012).
- [35] M. Leijnse and K. Flensberg, *Phys. Rev. B* **86**, 134528 (2012).
- [36] P. Recher, E. V. Sukhorukov, and D. Loss, *Phys. Rev. B* **63**, 165314 (2001).
- [37] L. Hofstetter, S. Csonka, J. Nygård, and C. Schönberger, *Nature (London)* **461**, 960 (2009).
- [38] L. G. Herrmann, F. Portier, P. Roche, A. L. Yeyati, T. Kontos, and C. Strunk, *Phys. Rev. Lett.* **104**, 026801 (2010).
- [39] G. Fülöp, F. Domínguez, S. d'Hollosy, A. Baumgartner, P. Makk, M. H. Madsen, V. A. Guzenko, J. Nygård, C. Schönberger, A. Levy Yeyati, and S. Csonka, *Phys. Rev. Lett.* **115**, 227003 (2015).
- [40] C.-X. Liu, G. Wang, T. Dvir, and M. Wimmer, *arXiv:2203.00107*.
- [41] S. V. Aksenov, A. O. Zlotnikov, and M. S. Shustin, *Phys. Rev. B* **101**, 125431 (2020).
- [42] N. Sedlmayr and C. Bena, *Phys. Rev. B* **92**, 115115 (2015).
- [43] N. Sedlmayr, J. M. Aguiar-Hualde, and C. Bena, *Phys. Rev. B* **93**, 155425 (2016).
- [44] T. Dvir, G. Wang, N. van Loo, C.-X. Liu, G. P. Mazur, A. Bordin, S. L. D. ten Haaf, J.-Y. Wang, D. van Driel, F. Zatelli, X. Li, F. K. Malinowski, S. Gazibegovic, G. Badawy, E. P. A. M. Bakkers, M. Wimmer, and L. P. Kouwenhoven, *arXiv:2206.08045*.
- [45] A. Brunetti, A. Zazunov, A. Kundu, and R. Egger, *Phys. Rev. B* **88**, 144515 (2013).
- [46] A. R. Wright and M. Veldhorst, *Phys. Rev. Lett.* **111**, 096801 (2013).
- [47] T. E. O'Brien, A. R. Wright, and M. Veldhorst, *Phys. Status Solidi B* **252**, 1731 (2015).
- [48] D. Stepanenko, M. Rudner, B. I. Halperin, and D. Loss, *Phys. Rev. B* **85**, 075416 (2012).
- [49] M. Governale, M. G. Pala, and J. König, *Phys. Rev. B* **77**, 134513 (2008).
- [50] A. V. Rozhkov and D. P. Arovas, *Phys. Rev. B* **62**, 6687 (2000).
- [51] Y. Tanaka, A. Oguri, and A. C. Hewson, *New J. Phys.* **9**, 115 (2007).
- [52] C. Karrasch, A. Oguri, and V. Meden, *Phys. Rev. B* **77**, 024517 (2008).
- [53] G. Wang, T. Dvir, G. P. Mazur, C.-X. Liu, N. van Loo, S. L. D. ten Haaf, A. Bordin, S. Gazibegovic, G. Badawy, E. P. A. M. Bakkers, M. Wimmer, and L. P. Kouwenhoven, *arXiv:2205.03458*.
- [54] See Supplemental Material at <http://link.aps.org/supplemental/10.1103/PhysRevB.106.L201404> including Refs. [73–77].
- [55] G. Kiršanskas, J. N. Pedersen, O. Karlström, M. Leijnse, and A. Wacker, *Comput. Phys. Commun.* **221**, 317 (2017).
- [56] D. I. Pikulin, B. van Heck, T. Karzig, E. A. Martinez, B. Nijholt, T. Laeven, G. W. Winkler, J. D. Watson, S. Heedt, M. Temurhan, V. Svidenko, R. M. Lutchyn, M. Thomas, G. de Lange, L. Casparis, and C. Nayak, *arXiv:2103.12217* v1.
- [57] J. Danon, A. B. Hellenes, E. B. Hansen, L. Casparis, A. P. Higginbotham, and K. Flensberg, *Phys. Rev. Lett.* **124**, 036801 (2020).
- [58] A. Pöschl, A. Danilenko, D. Sabonis, K. Kristjūhan, T. Lindemann, C. Thomas, M. J. Manfra, and C. M. Marcus, *arXiv:2204.02430* v1.
- [59] A. Maiani, M. Geier, and K. Flensberg, *Phys. Rev. B* **106**, 104516 (2022).
- [60] D. E. Liu, M. Cheng, and R. M. Lutchyn, *Phys. Rev. B* **91**, 081405(R) (2015).
- [61] D. E. Liu, A. Levchenko, and R. M. Lutchyn, *Phys. Rev. B* **92**, 205422 (2015).
- [62] S. Smirnov, *Phys. Rev. B* **99**, 165427 (2019).
- [63] G.-H. Feng and H.-H. Zhang, *Phys. Rev. B* **105**, 035148 (2022).
- [64] S. Smirnov, *Phys. Rev. B* **92**, 195312 (2015).
- [65] E. Sela, Y. Oreg, S. Plugge, N. Hartman, S. Lüscher, and J. Folk, *Phys. Rev. Lett.* **123**, 147702 (2019).
- [66] S. Smirnov, *Phys. Rev. B* **103**, 075440 (2021).
- [67] C. Han, Z. Iftikhar, Y. Kleeorin, A. Anthore, F. Pierre, Y. Meir, A. K. Mitchell, and E. Sela, *Phys. Rev. Lett.* **128**, 146803 (2022).
- [68] D. Aasen, M. Hell, R. V. Mishmash, A. Higginbotham, J. Danon, M. Leijnse, T. S. Jespersen, J. A. Folk, C. M. Marcus, K. Flensberg, and J. Alicea, *Phys. Rev. X* **6**, 031016 (2016).
- [69] R. S. Souto and M. Leijnse, *SciPost Phys.* **12**, 161 (2022).
- [70] P. Bonderson, M. Freedman, and C. Nayak, *Phys. Rev. Lett.* **101**, 010501 (2008).
- [71] K. Flensberg, *Phys. Rev. Lett.* **106**, 090503 (2011).
- [72] B. van Heck, A. R. Akhmerov, F. Hassler, M. Burrello, and C. W. J. Beenakker, *New J. Phys.* **14**, 035019 (2012).
- [73] K. F. H. Bruus, *Many-Body Quantum Theory in Condensed Matter Physics: An Introduction* (Oxford University Press, Oxford, 2004).
- [74] K. Grove-Rasmussen, G. Steffensen, A. Jellinggaard, M. H. Madsen, R. Žitko, J. Paaske, and J. Nygård, *Nat. Commun.* **9**, 2376 (2018).
- [75] Yu luh, *Acta Phys. Sin.* **21**, 75 (1965).
- [76] H. Shiba, *Prog. Theor. Phys.* **40**, 435 (1968).
- [77] A. I. Rusinov, *Sov. Phys. JETP Lett.* **9**, 85 (1969).